# **OPEN ACCESS**



# Trans-Neptunian Object Colors as Evidence for a Past Close Stellar Flyby to the Solar System

Susanne Pfalzner, Frank W. Wagner, and Paul Gibbon Jülich Supercomputing Center, Forschungszentrum Jülich, 52428 Jülich, Germany Received 2025 May 13; revised 2025 July 7; accepted 2025 July 8; published 2025 October 17

#### Abstract

Thousands of small bodies, known as trans-Neptunian objects (TNOs), orbit the Sun beyond Neptune. TNOs are remnants of the planets' formation from a disk of gas and dust, so it is puzzling that they move mostly on eccentric orbits inclined to the planetary plane and show a complex red-to-gray color distribution. A close stellar flyby can account for the TNOs' dynamics, but it is unclear if this can also explain the correlation between their colors and orbital characteristics. Assuming an initial red-to-gray color gradient in the disk, our numerical study finds that the spiral arms induced by the stellar flyby simultaneously lead to the observed TNOs' color patterns and orbital dynamics. The combined explanation of these TNO properties strengthens the evidence for a close flyby of another star to the young solar system. Our study predicts that (1) small TNOs beyond 60 au will mostly be gray, and (2) retrograde TNOs will lack the color most common to high-inclination TNOs. The anticipated TNO discoveries by the Vera Rubin telescope will be able to test these predictions. A confirmed flyby would allow us to reveal the chemical composition of the solar system's primordial disk.

Unified Astronomy Thesaurus concepts: Trans-Neptunian objects (1705) Materials only available in the online version of record: animation

#### 1. Introduction

More than 3000 subplanet-sized objects have been discovered beyond Neptune. These trans-Neptunian objects (TNOs) formed alongside the solar system's planets and provide valuable insight into the solar system's early history (B. Gladman & K. Volk 2021). Most TNOs are too faint for spectroscopic observations (N. Pinilla-Alonso et al. 2020; J. P. Emery et al. 2024; C. R. Glein et al. 2024), so their surface compositions are mainly studied through broadband photometry that reveals colors ranging from very red to bluegray (S. C. Tegler & W. Romanishin 1998; M. E. Brown 2012; M. A. Barucci & F. Merlin 2020).

The temperature decreases with increasing distance from the Sun, so one would expect the TNOs' colors to correlate with this distance too. However, no such relationship has been found (D. C. Jewitt & J. X. Luu 2001). Instead, the TNOs' colors appear to be related to their dynamic characteristics. Lowinclination and low-eccentricity TNOs in the cold Kuiper Belt are predominantly very red (S. C. Tegler & W. Romanishin 2000; O. R. Hainaut & A. C. Delsanti 2002; A. Doressoundiram et al. 2005; N. Peixinho et al. 2008), while TNOs in the hot Kuiper Belt moving on inclined, eccentric orbits exhibit a mix of red and gray tones. Recent surveys, such as the Outer Solar System Survey (OSSOS; M. E. Schwamb et al. 2019), Dark Energy Survey (DES; P. H. Bernardinelli et al. 2023), and James Webb Space Telescope (N. Pinilla-Alonso et al. 2025), indicate that very red TNOs are rare at inclinations,  $i > 21^{\circ}$  (M. Marsset et al. 2019), and eccentricities, e > 0.42 (M. Ali-Dib et al. 2021). The underlying reason for these correlations is unclear.

Here, we investigate a close flyby of another star as a possible reason for the correlations between color and

Original content from this work may be used under the terms of the Creative Commons Attribution 4.0 licence. Any further distribution of this work must maintain attribution to the author(s) and the title of the work, journal citation and DOI.

dynamics. Specifically, we consider a  $0.8 M_{\odot}$  star passing at a periastron distance  $r_P = 110$  au with an inclination  $i_P = 70^{\circ}$ . This flyby reproduces the dynamics of currently known TNOs remarkably well (S. Pfalzner et al. 2024a). The question is whether this flyby can also account for the observed color distribution of the known TNOs.

# 2. Method

We simulate the effect of the flyby of a  $0.8\,M_\odot$  star on a disk modeled with 10,000 and 50,000 massless test particles initially orbiting the Sun on Keplerian trajectories. The size of the primordial solar disk is unknown. Observed sizes of protoplanetary and debris disks typically range from 100 to 500 au (S. M. Andrews 2020; N. Hendler et al. 2020). We model the effect of a flyby up to a radius of 150 au. The results for smaller-sized disks are contained as a subset of the results' data (see Appendix A). We model the disk by an initially constant test particle surface density. The reason is that the outer disk areas are better resolved with such an approach. In the second step, one can assign different masses to the particles to model the actual mass density (S. M. Hall 1997; M. Steinhausen et al. 2012; S. Pfalzner et al. 2024a). Appendix B contains examples for 1/r- and  $1/r^{3/2}$ -dependent initial surface densities.

We assume a color gradient in the preflyby disk and represent it by a rainbow color spectrum between 30 and 150 au, as illustrated in Figure 1(a). The cold Kuiper Belt objects move on near-circular orbits close to the plane. It is generally assumed that these cold Kuiper Belt objects remained close to their place of origin (A. H. Parker & J. J. Kavelaars 2010; J. M. Petit et al. 2011; W. C. Fraser et al. 2021). These bodies are nearly exclusively very red in color (A. Thirouin & S. S. Sheppard 2019; W. C. Fraser et al. 2021; P. H. Bernardinelli et al. 2025). Therefore, we assume that the primordial disk was dominated by very red bodies in the cold Kuiper Belt region and that beyond this objects of various

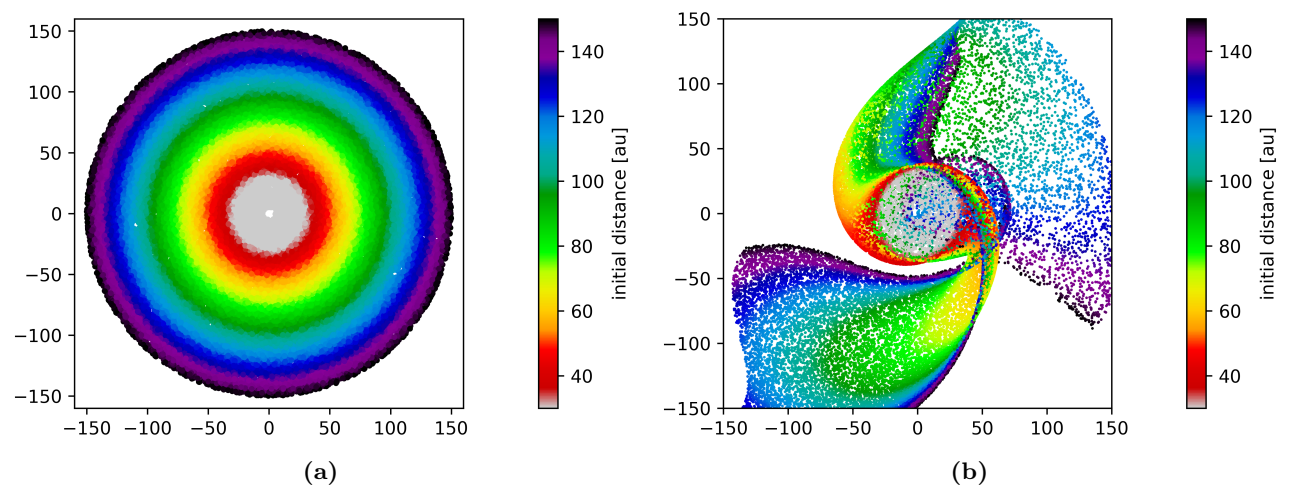


**Figure 1.** Effect of flyby. (a) The preflyby color gradient in the simulated disk is depicted by a false color scheme representing very red to blue–gray TNOs. The same color scheme is used throughout the Letter. (b) Simulation snapshot of the flyby 128 yr after periastron passage. The perturber star approached from the bottom right and already left the shown area. Disk matter is transported inward and outward along the spiral arms, with a fraction of the test particles injected into the planet region. Only the particles remaining bound to the Sun are shown. The movie shows how the flyby induces the formation of spiral arms, eventually leading to observed color mixing within the disk. The disk has initially a radius of 150 au. The movie covers the time up to 12,000 yr after periastron passage. (An animation of this figure is available in the online article.)

shades of gray existed. Our rainbow color representation of this situation has two functions. First, it is a temporary placeholder for the observed slope *S* and will eventually link to the TNOs' compositions. Second, it links to the primordial disk size. One can locate which particles would be absent if the primordial disk were smaller than 150 au.

The perturber star ( $M_P = 0.8 \, M_\odot$ ) approached a periastron distance  $r_P = 110 \, \mathrm{au}$  on an inclined orbit  $i_P = 70^\circ$  with an argument of periastron  $\omega_P = 80^\circ$ . The flyby probably took place during the early phases of the solar system in the Sun's birth cluster. In such clusters, the stellar density is about 1000 to 1,000,000 times higher than the local stellar density, and therefore, close flybys are much more common. Due to the stars in a young cluster being almost coeval, most flybys happen on nearly parabolic orbits even in dense stellar groups, such as the Orion Nebula cluster (C. Olczak et al. 2010). At least 140 million solar-type stars in the Milky Way may have experienced a similar flyby in their youth (S. Pfalzner et al. 2024a).

A flyby with the above parameters effectively reproduces all the known dynamic groups among the TNOs (S. Pfalzner et al. 2024a) apart from the resonant populations, which appear later on through interactions with Neptune. The disk's response is modeled using the REBOUND code (H. Rein & D. S. Spiegel 2014) with the IAS15 integrator. This *N*-body approach is sufficient as the gas mass in the debris disk is negligible (e.g., H. Kobayashi & S. Ida 2001; Z. E. Musielak & B. Quarles 2014; S. Pfalzner et al. 2018). For more detailed information on the simulation method, see S. Pfalzner et al. (2024b). The perturber's influence on test particle orbits becomes negligible approximately 12,000 yr after periastron passage.

To study the long-term evolution after the flyby, we use the GENGA code (S. L. Grimm & J. G. Stadel 2014; S. L. Grimm et al. 2022) with its hybrid symplectic integrator (J. E. Chambers 1999). Here, we also consider the interactions with the four giant planets of the solar system. We limited our simulations to the first 1 Gyr after the flyby because the computational cost remains relatively high despite the high numerical efficiency of GENGA. We find a time step of  $\Delta t = 23$  days is sufficient to obtain the required temporal resolution.

#### 3. Results

We simulate the effect of the stellar flyby on a debris disk. We assume a color gradient as illustrated in Figure 1(a). The color gradient is used as a temporary placeholder for the observed slope *S*. During the flyby, some TNOs become unbound, while others are captured by the perturber. However, most remain bound to the Sun (S. Pfalzner et al. 2024a). The perturber significantly alters their orbits, creating visible spiral arms due to the induced sub- and super-Keplerian velocities (Figure 1(b)). The sub-Keplerian stream moves planetesimals inward (dark blue), whereas the super-Keplerian stream pushes particles outward (red/yellow; S. Pfalzner 2003).

Colors are primarily known for relatively close TNOs (B. Gladman & K. Volk 2021), mostly from the Kuiper Belt region. However, these TNOs represent only a portion of the entire population of discovered TNOs. In addition, the real number of TNOs likely very much exceeds that of the known TNOs. For example, the number of undiscovered detached TNOs (a > 47.2 au, e > 0.42) is expected to exceed that of the currently known Kuiper Belt population (B. Gladman & K. Volk 2021). For our comparison with the observations, we focus on TNOs with p < 60 au and  $i < 50^{\circ}$ . By contrast, we look at the extended parameter space for predictions of future discoveries. An illustration of the entire parameter space is given by Figures A1(a) and (b) of the Appendix.

#### 3.1. Inclination Correlation

Figure 2 illustrates the relationship between the TNOs' colors, inclinations, and periastron distances, comparing the OSSOS observations in the left column to our simulations on the right. M. Marsset et al. (2019) analyzed the colors of 229 TNOs on dynamically excited orbits from the OSSOS survey. They find that very red objects are rare at inclinations  $i > 21^{\circ}$  (see Figure 2(a)). Figure 2(c) shows the corresponding distributions. M. Marsset et al. (2019) classified TNOs as red (S > 20.4) or gray (S < 20.4) based on spectral slope S, as indicated by the gray dashed lines. Note the inverted x-axes, chosen for a better comparison with the simulations.

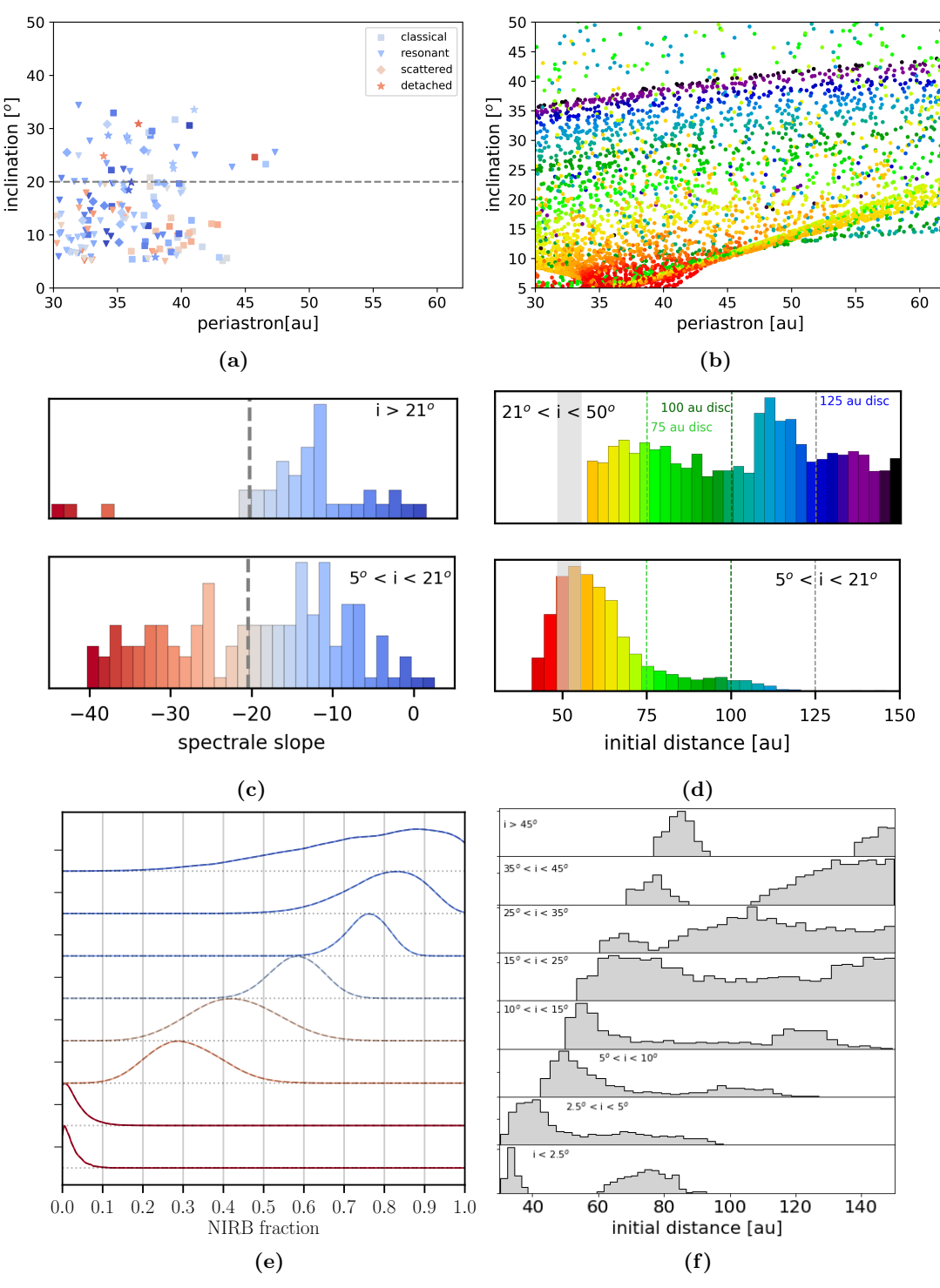


Figure 2. Connection between TNO color and inclination. The left column illustrates the observational data of M. Marsset et al. (2019) and P. H. Bernardinelli et al. (2025), and the right column shows the numerical results from our flyby simulation. The top row displays scatter plots of the TNOs' inclination as a function of periastron distance. The middle row shows color distributions for the high-inclination ( $i > 21^{\circ}$ ) and the low-inclination ( $5^{\circ} < i < 21^{\circ}$ ) objects, respectively. The colors in panels (b) and (d) indicate the distance to the Sun in the preflyby disk as defined in Figure 1(a). The colors can also be used to convert the results to smaller initial disk sizes. The vertical lines in panel (c) correspond to the gray area in panel (d) and show the border between very red and gray TNOs in the observations and simulations. For the data of M. Marsset et al. (2019) we excluded the centaurs. (e) Observations of the fraction of infrared bright objects as a function of inclination bin for the classical TNOs in the DES survey (P. H. Bernardinelli et al. 2025). (f) Simulation results of the origin distribution for the same inclination bins. Only objects with 30 au are considered.

The simulations reflect similar findings: red test particles are mainly found at low inclinations and periastron distances, suggesting that they retain more of their original dynamics. In contrast, green to blue objects dominate at higher inclinations,

with red and orange particles being rare (see, Figures 2(b) and (d)). The red test particles correspond to the very red TNOs, whereas the other colors represent the shades of gray observed for TNOs. Red TNOs appear to be more common at periastron

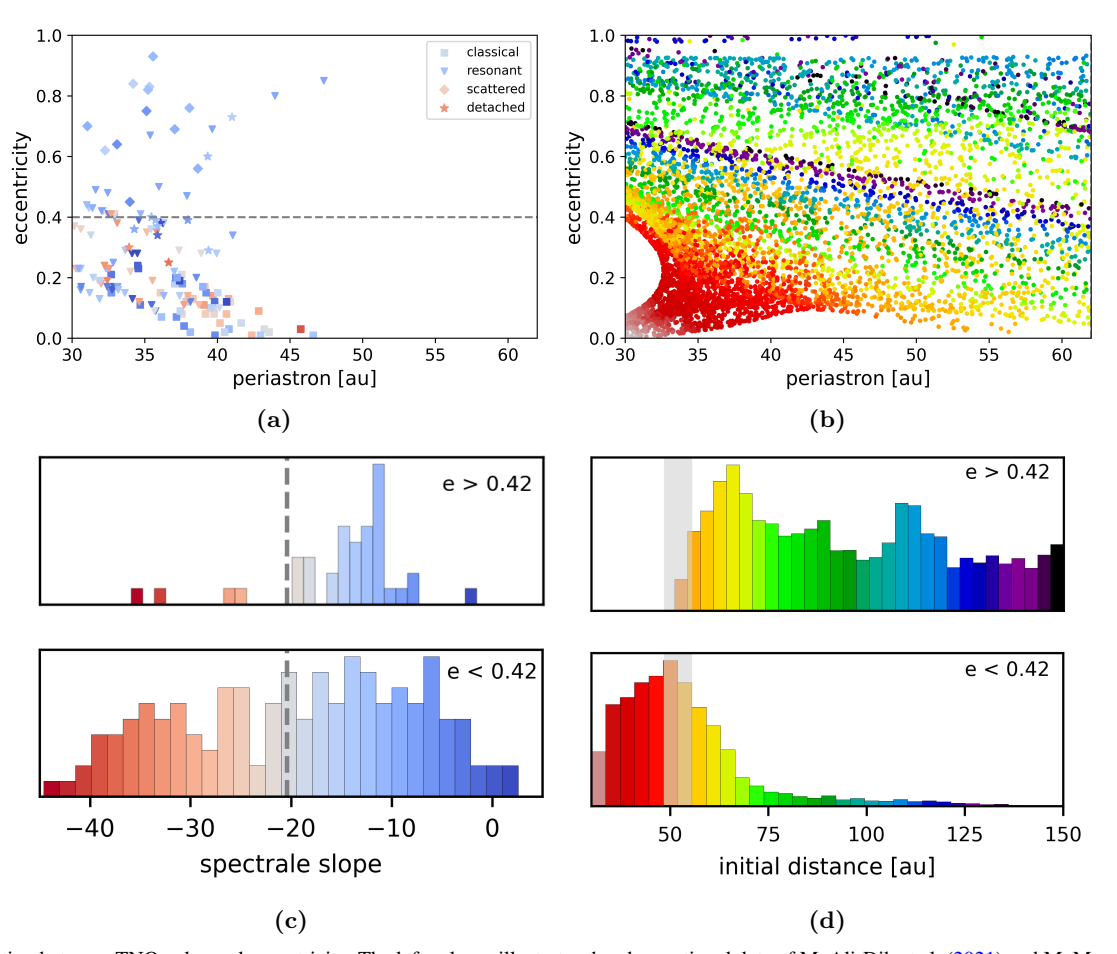


Figure 3. Connection between TNO color and eccentricity. The left column illustrates the observational data of M. Ali-Dib et al. (2021) and M. Marsset et al. (2019), and the right column shows the numerical results from our flyby simulation. Panels (a) and (b) display scatter plots of the TNOs' eccentricity as a function of periastron distance. Panels (c) and (d) show the corresponding color distributions distinguishing between objects with e > 0.42 and e < 0.42. The colors in panels (b) and (d) are as defined in Figure 1(a). For the data of M. Marsset et al. (2019) we excluded the centaurs.

distances 35 au, although this could be affected by the low number of TNOs with <math>p > 45 au. The gray bars correspond roughly to the gray dashed lines in Figure 2(c). The simulation data are available via doi:10.26165/JUELICH-DATA/9Z9K47 and doi:10.26165/JUELICH-DATA/LGBORQ.

Figures 2(b) and (d) can also be used to infer the results for smaller-sized disks. In Figure 2(d), we indicated where the distribution would end for disks of size 75, 100, and 125 au, respectively. For Figure 2(b), one has to subtract the corresponding colors from the plot. We illustrate this process for a 100 au sized system by Figure A1(c) of the Appendix. In the Appendix, we also show that the result of the black of red objects at high inclinations is valid not only for the test particle distribution shown here, but also for 1/r (blue) and  $1/r^{3/2}$  (red) surface distributions in the preflyby disk (see, Figure B1).

The consistency of these observed trends is further supported by P. H. Bernardinelli et al. (2025)'s analysis of 697 TNOs from DES, which confirmed the OSSOS findings. They classified TNOs into two groups: "near-IR bright" (NIRB) and "near-IR faint" (NIRF), revealing a systematic shift in their ratio with higher inclinations (see Figure 2(e)). Our simulations (Figure 2(f)) also show this change, with a surprising degree of match despite the approximate color definition. Even the slightly backward trend toward redder

colors in the  $40^{\circ}$ – $60^{\circ}$  range is evident. However, here, the statistics are less robust than in the other inclination intervals.

# 3.2. Eccentricity Correlation

We examine the correlation between the colors of TNOs and their orbital eccentricities. M. Ali-Dib et al. (2021) found a lack of very red TNOs for those with e>0.42 (Figure 3(a)). This scarcity is clearly visible when comparing the spectral index distributions for TNOs with e>0.42 (Figure 3(c), top) with those for TNOs with e<0.42 (Figure 3(c), bottom).

Our simulations (Figures 3(b) and (d)) mirror this trend, showing few red particles at high eccentricities (e>0.42). Figure A1(d) of the Appendix illustrates that this match is also obtained for a 100 au sized disk. High-eccentricity TNOs originate primarily from the outer disk, injected into high-inclination orbits, while low-eccentricity TNOs remain close to their origins. Thus, the flyby model simultaneously explains the scarcity of red objects at high inclination and at high eccentricity. We also conclude that the orbits of the few nonred TNOs among the low-eccentricity TNOs result from recircularization due to the long-term evolution.

In the observation and simulation scatter plots (Figures 3(a) and (b)), a decline in the periastron distance of the maximum eccentricity for red objects may be apparent, but more observational data are required to confirm this additional similarity.

https://destiny.fz-juelich.de

In summary, the suggested flyby provides a simple explanation for the connection between color and inclination. Its simplicity is the strong point of this model. Generally, highly inclined flybys lift the population outside the red-cold Kuiper Belt region to high inclinations and eccentricities. Given the complexity of the color redistribution (Figure 1(b)), the more subtle features are sensitive to flyby parameters. Not every flyby leads to the observed color pattern. For example, closer flybys or a higher perturber mass would lift the test particles of the cold Kuiper Belt region to high inclination and eccentricities' mixing of red and blue colors in the Kuiper Belt region. Less inclined flybys would lead to less lifting out of the plane. The clear division would disappear in both cases and shift to other locations.

## 3.3. Colors of Dynamic Groups

The fraction of red TNOs varies among dynamic groups. Early observations indicated that the cold population is predominantly very red, whereas the hot population displays various colors (S. C. Tegler & W. Romanishin 2000; O. R. Hainaut & A. C. Delsanti 2002; A. Doressoundiram et al. 2005; N. Peixinho et al. 2008). According to M. Marsset et al. (2019), only 8% of classical TNOs are very red, compared to 36% of resonant TNOs. However, the orbits of resonant and scattered disk objects likely changed in the past by interacting with Neptune.

We concentrated on populations least influenced by the interactions with Neptune. Detached objects, defined as nonresonant TNOs with a > 47.4 au and e > 0.24 (B. Gladman & K. Volk 2021), are such a group. M. Marsset et al. (2019) observed that only 2 of the 13 detached TNOs are very red, leading to a rate of <10% for such objects (excluding the centaur 2007 JK43). In the DES sample, P. H. Bernardinelli et al. (2025) found radial stratification within the NIRB population, in that hot Kuiper Belt objects NIRFs are on average redder than detached NIRBs. Our flyby simulation reproduces the scarcity of red objects among detached TNOs, which is explained by detached objects primarily originating from the 55 to 70 au region. We also replicate the trend of increasing orbital inclinations from light red to gray in the color distribution identified by M. Marsset et al. (2023). Thus, our simulations also recover trends among subgroups of the sample, summarized in Figure C1 in the Appendix.

# 3.4. Long-term Evolution

Interactions with the planets have affected the orbits of some TNOs, particularly those close to Neptune. We only modeled the first Gyr postflyby due to the computational demands of tracking tens of thousands of test particles over long periods.

After 1 Gyr, the overall structure is similar, with very red objects remaining rare among high-inclination and high-eccentricity TNOs. However, the color patterns become less distinct (Figures 4(a) and (b)), as some red particles shift to high-inclination orbits or are ejected, especially those with 30 au, low inclinations, and low eccentricities.

The distinct differences in the color distributions between low- and high-inclination, as well as low- and high-eccentricity, TNOs persist (Figures 4(c) and (d)). The alignment between observations and simulations is maintained even after this long period. We find that interactions with Neptune are most intense

in the first 100 Myr, with diminished effects afterward, indicating that the color patterns will persist over even longer timescales. On the dynamic side, the most significant impact of the long-term evolution is the emergence of TNOs on resonant orbits.

### 3.5. Prediction for LSST Discoveries

LSST is projected to increase the number of detected TNOs tenfold, allowing for color and spectral analysis. In anticipation of this, we try to predict the colors of these soon-detectable TNOs from a flyby perspective. Focusing on distant TNOs with 60 au (see Figures 5(a) and (b)), we find that the test particle colors range from yellow to dark blue, with very few red objects, regardless of inclination or eccentricity. This translates into distant TNOs predominantly being light red to various shades of gray and a notable lack of very red objects, even among low-inclination and low-eccentricity TNOs. These TNOs (<math>60 au) are mainly transported inward from regions between 65 and 150 au.

We also predict that the color distribution of retrograde TNOs differs significantly from prograde TNOs (Figures 5(c) and (d)). They even differ from the high-inclination prograde ones ( $60^{\circ} < i < 90^{\circ}$ ), which are mostly medium gray, since they originate from 80 to 110 au. In contrast, retrograde TNOs originate from two distinct regions (70–90 au and 120–150 au), showing a bimodal distribution of light-red and predominantly dark-gray to blue–gray colors. The retrograde TNOs lack the colors most common for high-inclination TNOs. Thus, the colors of the retrograde TNOs could provide an even more rigorous test of this model and other hypotheses.

#### 3.6. Connection to Irregular Moons

A further argument for a stellar flyby is based on the colors of the irregular moons. It has long been speculated that irregular satellites originate from the same planetesimal reservoir as the TNOs, possibly being captured from regions beyond Neptune shortly after the giant planets formed (D. Jewitt & N. Haghighipour 2007). A capture would explain the distinct characteristics of irregular moons, such as orbiting their host planets in more distant, inclined, and eccentric orbits than regular moons. However, there exists one difference to the TNOs—the irregular lack of very red objects.

Several hypotheses exist about how the TNOs moved from beyond Neptune into the region of the giant planets (D. Nesvorný et al. 2014). We suggested recently that a stellar flyby could inject TNOs into the vicinity of the giants (S. Pfalzner et al. 2024b). For our flyby parameters, all injected TNOs come from beyond 60 au, explaining the observed lack of very red objects (see Figure D1 in the Appendix). Reanalyzing the injected TNOs, we find that their colors should resemble those of high-inclination TNOs shown in Figure 2. Thus, the stellar flyby could explain both the TNOs' color distribution and the scarcity of highly red objects among the irregular moons.

# 4. Discussion

# 4.1. Selection Effects and Color Evolution

Comparing simulations and observations is influenced by several biases. The faintness of TNOs limits detections to larger and brighter objects (M. T. Bannister et al. 2018). Additionally, TNOs with large perihelion distances and those

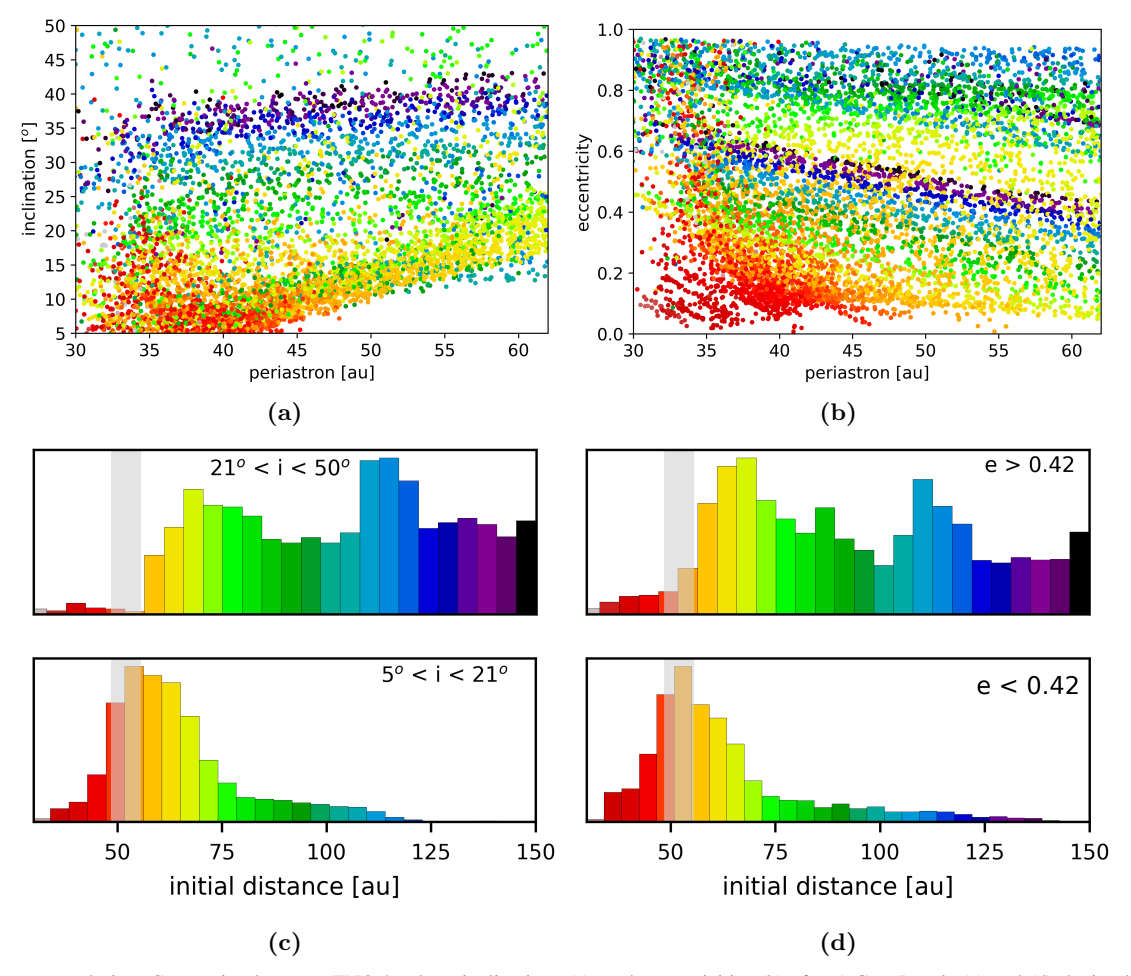


Figure 4. Long-term evolution. Connection between TNOs' colors, inclinations (a), and eccentricities (b) after 1 Gyr. Panels (c) and (d) depict the corresponding color distributions.

on highly eccentric or inclined orbits are often underrepresented (e.g., J. M. Petit et al. 2017). In addition, if TNO colors are related to size or orbital parameters, these biases impact the comparison between observations and models.

We showed that for our flyby scenario a primordial disk dominated by very red bodies in the cold Kuiper Belt region and objects of various shades of gray beyond 50 au can reproduce the observed color. However, it is unclear how this is related to the chemical composition of the primordial disk. There are two reasons for this uncertainty: First, the link between the chemical compositions of TNOs and their colors is not fully understood. Second, it is unclear to what extent the surface differs from the bulk compositions of TNOs. Factors such as UV irradiation, cosmic rays, and particle impacts may have altered the surfaces of TNOs (M. E. Brown et al. 2011). Unfortunately, the chemical distribution in observed disks cannot solve this problem. Theoretically, disk stratification is believed to be the result of the position of snowlines. However, actual disk observations reveal considerable variation in material distribution within disks (K. I. Öberg et al. 2023), which challenges the idea that snowlines are the only factor influencing a disk's chemical structure (G. Perotti et al. 2023). The complexity of TNO and disk chemistry makes it difficult to identify the dominant processes that could have led to a redto-gray stratification in the solar system's disk.

For irregular moons, the situation is even more complex. Outgassing of volatile materials (D. Jewitt & N. Haghighipour 2007; D. Jewitt 2018) or collisional breakup (E. Ashton et al. 2021) may have also altered their appearance.

# 4.2. Comparison to Planet Instability Model

Several other models attempt to explain the dynamics of TNOs (e.g., L. Jílková et al. 2015; G. Brown et al. 2024; D. Vokrouhlický et al. 2024), but only the planet instability model has explored the connection between TNO dynamics and their colors to date. This model posits that TNOs originate from the region between the giant planets, were ejected due to planet migration, and some were recaptured in the outer solar system (e.g., J. A. Fernandez & W. H. Ip 1984; J. M. Hahn & R. Malhotra 1999; A. Morbidelli et al. 2003; H. F. Levison et al. 2008; S. N. Raymond et al. 2020). While this effectively accounts for classical Kuiper Belt objects, it requires additional mechanisms to account for TNOs with retrograde or Sedna-like orbits.

Planet instability studies on TNO colors (D. Nesvorný et al. 2020; M. Ali-Dib et al. 2021) suggest a gray population close to the Sun and a red population farther out. The model indicates that the planet instability alters the TNO orbits, mixing these populations, with the resulting color distribution depending on the initial color divide and the type of Neptune's migration (e.g., M. E. Brown et al. 2011; D. Nesvorný et al. 2020).

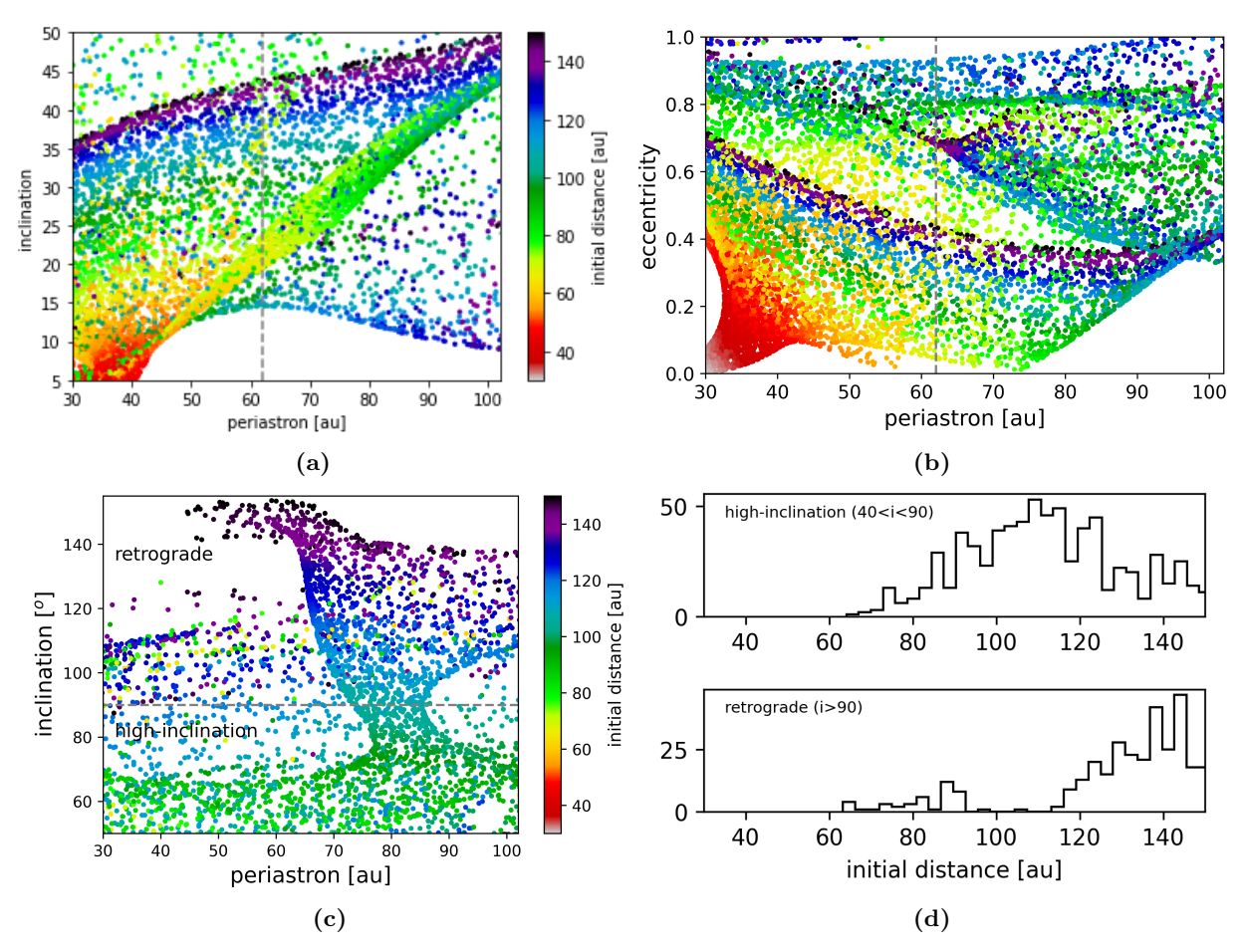


Figure 5. Predictions for LSST. Panels (a) and (b) for TNOs with perihelion distances exceeding 60 au. Panel (c) shows the colors of highly inclined and retrograde objects with p < 100 au. Panel (d) illustrates the corresponding color distributions.

M. Ali-Dib et al. (2021) found color transitions at 38 or 42 au could explain the scarcity of very red TNOs at high inclinations. However, a 38 au transition overrepresents very red scattered disk objects, while a 42 au transition underrepresents very red plutinos, indicating that the link between TNO dynamics and colors remains unresolved.

# 5. Conclusion

We investigated whether the close flyby of a perturbing star  $(M_P = 0.8 \, M_\odot, r_P = 110 \, \text{au}, i_P = 70^\circ)$  could explain the complex color distribution of the TNOs. Assuming an initial color gradient in the Sun's debris disk, we found that the flyby accounts simultaneously for the observed color correlations from the OSSOS and DES surveys. Specifically, those very red TNOs:

- 1. become increasingly scarce for higher inclinations ( $i > 21^{\circ}$ ),
- 2. are rare among very eccentric (e > 0.42) TNOs,
- 3. and within the detached population.

We also reproduce the trend of increasing inclinations toward the bluer end of the color distribution of bright infrared object. We connect it to the transport in spiral arms created during the flyby. The long-term evolution over 1 Gyr changes the color structure only slightly.

This simultaneous explanation of the TNO dynamics and colors significantly strengthens the argument for a stellar flyby

largely determining the structure of the solar system beyond Neptune. Moreover, the dynamics and colors of the irregular moons can also be accounted for (S. Pfalzner et al. 2024b).

Upcoming instruments like LSST are expected to detect tens of thousands of new TNOs. We predict that (1) distant TNOs will mainly be gray to blue–gray, unless they are dwarf planets; (2) retrograde TNOs will show a bimodal color distribution, with some light-red objects and a distinct blue–gray group, but lacking the color most common among high-inclination TNOs; and (3) the inclination versus periastron correlation will reveal stripes of blue–gray TNOs at high inclinations. These predictions can be tested within 3 yr, potentially confirming the flyby hypothesis and clarifying its influence on the outer solar system.

#### Acknowledgments

The authors thank Pedro Bernardinelli for the valuable discussions on the DES results. We would also like to thank the referee for the very useful comments and suggestions, which have helped to improve the quality of the manuscript. Our appreciation further extends to the editor for the efficient handling of our submission. The simulations were performed on the JUWELS and JURECA supercomputers at the Jülich Supercomputing Center.

#### **Author Contributions**

Conceptualization, S.P.; simulation of the flyby and long-term evolution, F.W.; diagnostic: S.P., P.G.; comparison to observational data, S.P.; writing, S.P., F.W., P.G.; data curation, F.W.

# Appendix A Entire Parameter Space and Dependence on Disk Size

In the main part of the Letter, we concentrate on the parameter space accessible by observations. The complete parameter space showing the resulting correlation between TNOs' colors and their dynamical parameters is illustrated in Figures A1(a) and (b). Panels (a) and (b) show the inclinations and eccentricities of the TNOs as functions of periastron distance, respectively. The symbol colors indicate the TNOs' origin in the preflyby disk. The red color corresponds to the red TNOs, whereas the other colors represent the shades of gray observed for the TNOs. The red TNOs concentrate at low inclinations, eccentricities, and periastron distances. This reflects the fact that they retain much more of their original dynamics than particles at larger distances from the Sun.

The emerging pattern reflects the two primary spiral arms that form during the flyby, along with some less pronounced higher-order arms. In the spiral arms, two adjacent streams of planetesimals with different velocities form—one with sub-, the other with super-Keplerian velocities. The sub-Keplerian stream moves particles inward, while the super-Keplerian stream pushes planetesimals outward (S. Pfalzner 2003). An example of this effect can be seen in the dark-blue stripes of the inclination–periastron plot (see, Figure A1(a)). These particles were originally located beyond 100 au and have moved inward along the edges of the spiral arms.

A large unknown is the disk size before the flyby. Here we show the result for up to 150 au sized disks. The rainbow color plate can be used to illustrate the result for smaller disks. Figures A1(c) and (d) show the results for the example of a 100 au preflyby disk. The parameter space would lack the blue particles in the scatter plots of Figure 2(b) and 3(b). Equivalently, the plots of the distributions would simply stop at 100 au. The general result of the lack of very red objects among high-inclination and high-eccentricity TNOs is largely insensitive to disk size as long as it exceeds 70 au.

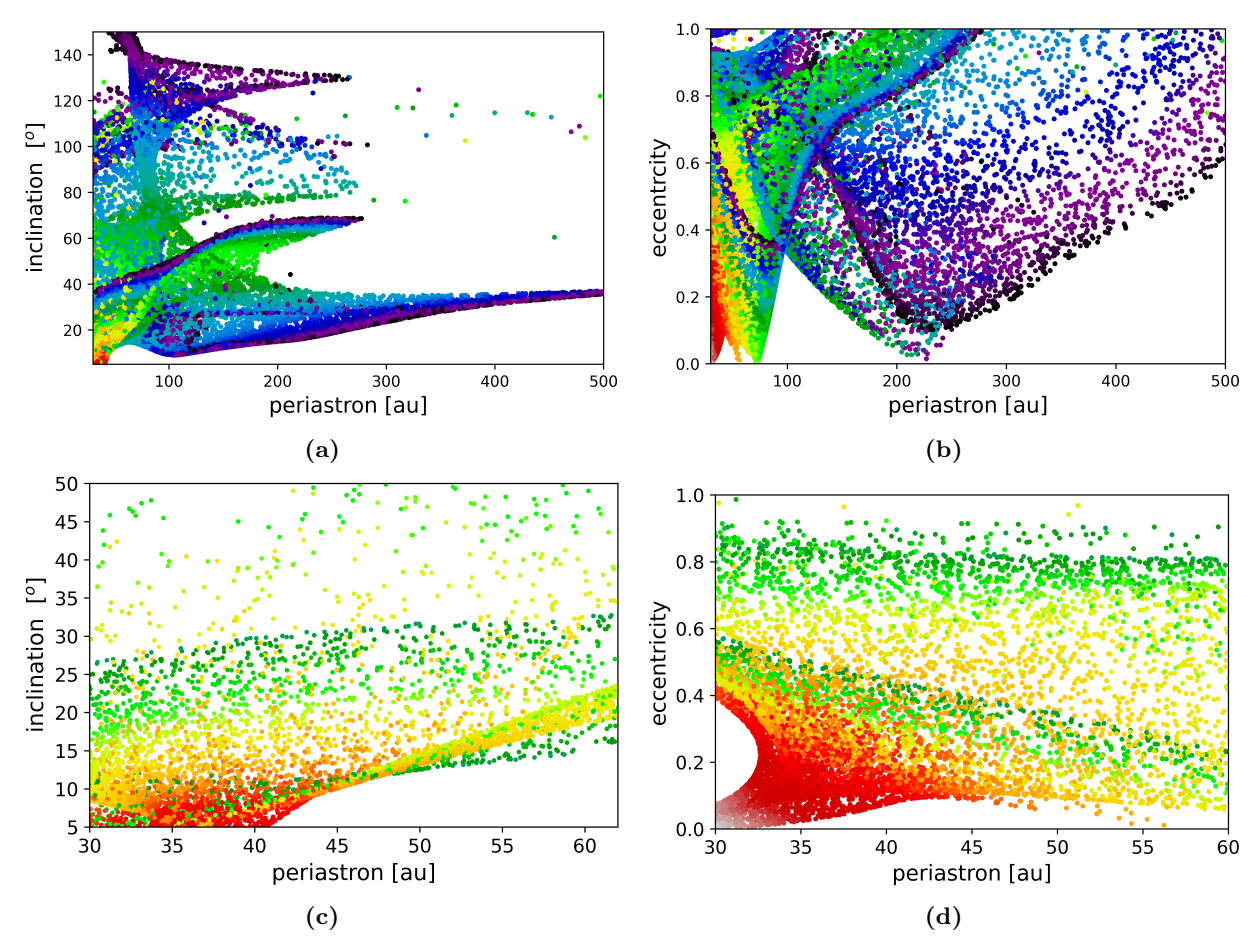
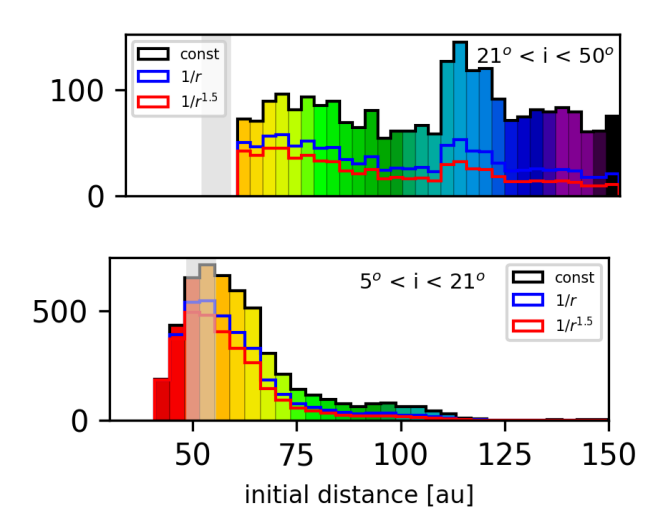


Figure A1. Entire parameter space and 100 au sized disk. Scatter plot of the TNOs' inclinations as a function of perihelion distance for (a) the entire parameter space and (c) a 100 au sized disk. Scatter plot of the TNOs' eccentricities as a function of perihelion distance for (b) the entire parameter space and (d) a 100 au sized disk.

# Appendix B Dependence on Surface Density in Preflyby Disk

The surface density distribution in the preflyby disk is unknown. In the main part of the Letter, we show the test particle density. The result for a given surface density is obtained by assigning different masses to the test particles (S. M. Hall 1997;

M. Steinhausen et al. 2012; S. Pfalzner et al. 2024a). Figure B1 compares the inclination distributions similar to Figure 2(d) for constant, 1/r-dependent, and  $1/r^{3/2}$ -dependent initial surface densities. It shows that the general result of a relative lack of very red TNOs at high-inclination TNOs remains valid. However, the density of distant TNOs is lower for steeper surface densities.



**Figure B1.** Surface density dependence. Origin of the high- and low-inclination TNOs as in Figure 2(d). However, here we show a comparison of the test particle distribution (black), with those assuming a 1/r (blue) and a  $1/r^{3/2}$  (red) surface distribution in the preflyby disk.

### Appendix C Detached TNOs

B. Gladman & K. Volk (2021) define detached objects as a nonresonant TNO with a > 47.4 au and e > 0.24. The data presented by M. Marsset et al. (2019) confirmed earlier results, which hinted at a scarcity of very red objects among detached TNOs. They find that only 2 out of their 13 detached objects exhibit red colors (see Figure C1(a), top). One of the red objects (2007 JK43) has a periastron distance of less than 30 au, which would not be included in the diagnostics in our simulations. Thus, the rate of very red detached objects is <10%. In the DES sample, detached TNOs are consistent with about 70% being gray. P. H. Bernardinelli et al. (2025) also

find evidence for radial stratification within the primordial NIRB population, with hot Kuiper Belt object NIRBs being, on average, redder than detached NIRBs.

Our flyby simulation reproduces the trend of a scarcity of red objects among detached TNOs. The simulation results indicate that the detached objects originate primarily from the region 50 to 55 au (see Figure C1(a), bottom). Consequently, gray objects dominate over red TNOs significantly in the detached population, and red objects are scarce. M. Marsset et al. (2023) identified a trend of increasing orbital inclinations from the lightly red to the gray end of the color distribution, both in the optical and near-infrared. Our simulation also recovers this trend (see Figure C1(b)).

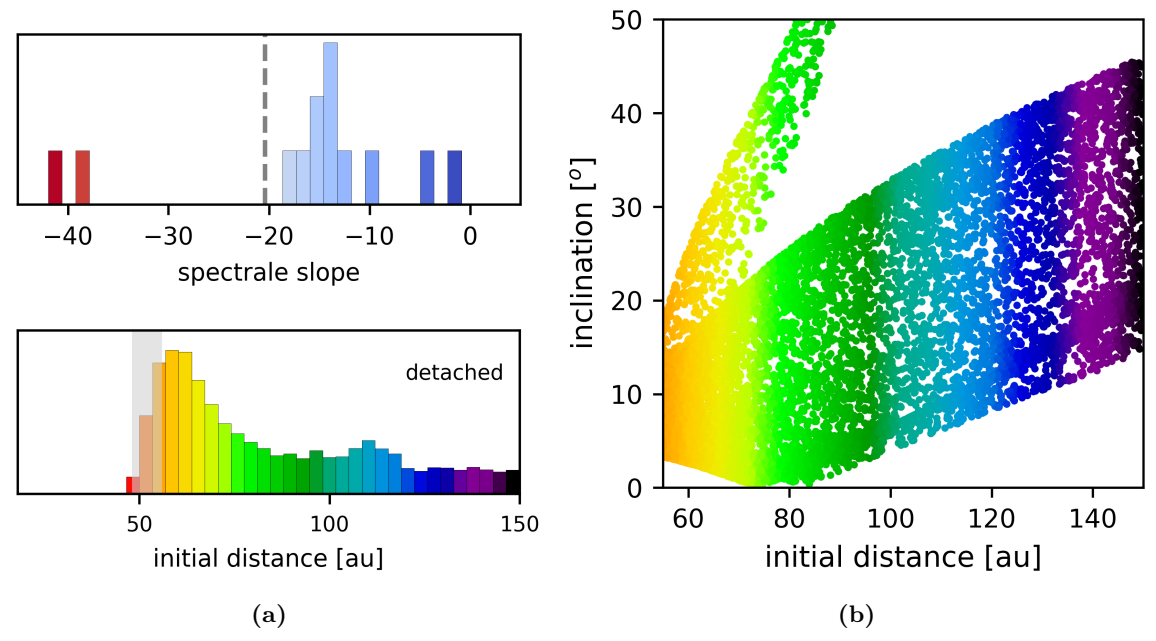
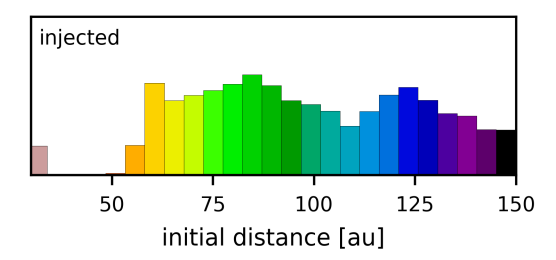


Figure C1. Other correlations between colors and dynamical parameters. Panel (a) illustrates the scarcity of very red objects among the detached TNOs in the observations (top) and simulations (bottom). Panel (b) depicts the inclination as a function of the initial distance of the TNOs.

### Appendix D Injected TNOs

In the stellar flyby modeled here, all the injected TNOs originate from beyond 60 au. Figure D1 shows the origin distribution of the injected TNOs. It shows the expected scarcity of very red objects. Furthermore, it resembles to a high degree the distribution we found for the high-inclination  $(i > 21^{\circ})$  TNOs shown in Figure 2. Therefore, we also expect their color distribution to match. Consequently, the stellar flyby would not only account for the TNOs' color distribution but also explain the observed absence of highly red objects among the irregular moons. This scarcity of very red objects would directly result from the origin of the injected TNOs in the outer areas of the disk.



**Figure D1.** Injected TNOs. Origin distribution of TNOs injected within 29 au, which may have been partly captured as irregular moons.

#### **ORCID iDs**

Susanne Pfalzner https://orcid.org/0000-0002-5003-4714 Frank W. Wagner https://orcid.org/0009-0001-5904-1742 Paul Gibbon https://orcid.org/0000-0002-5540-9626

# References

Ali-Dib, M., Marsset, M., Wong, W.-C., & Dbouk, R. 2021, AJ, 162, 19
Andrews, S. M. 2020, ARA&A, 58, 483
Ashton, E., Gladman, B., & Beaudoin, M. 2021, PSJ, 2, 158
Bannister, M. T., Gladman, B. J., Kavelaars, J. J., et al. 2018, ApJS, 236, 18
Barucci, M. A., & Merlin, F. 2020, in The Trans-Neptunian Solar System, ed.
D. Prialnik, M. A. Barucci, & L. Young (Amsterdam: Elsevier), 109
Bernardinelli, P. H., Bernstein, G. M., Abbott, T. M. C., et al. 2025, AJ, 169, 305
Bernardinelli, P. H., Bernstein, G. M., Jindal, N., et al. 2023, ApJS, 269, 18
Brown, G., Malhotra, R., Rein, H., et al. 2024, arXiv:2412.04583

```
Brown, M. E. 2012, AREPS, 40, 467
Brown, M. E., Schaller, E. L., & Fraser, W. C. 2011, ApJL, 739, L60
Chambers, J. E. 1999, MNRAS, 304, 793
Doressoundiram, A., Peixinho, N., Doucet, C., et al. 2005, Icar, 174, 90
Emery, J. P., Wong, I., Brunetto, R., et al. 2024, Icar, 414, 116017
Fernandez, J. A., & Ip, W. H. 1984, Icar, 58, 109
Fraser, W. C., Benecchi, S. D., Kavelaars, J. J., et al. 2021, PSJ, 2, 90
Gladman, B., & Volk, K. 2021, ARA&A, 59, 203
Glein, C. R., Grundy, W. M., Lunine, J. I., et al. 2024, Icar, 412, 115999
Grimm, S. L., & Stadel, J. G. 2014, ApJ, 796, 23
Grimm, S. L., Stadel, J. G., Brasser, R., Meier, M. M. M., & Mordasini, C.
  2022, ApJ, 932, 124
Hahn, J. M., & Malhotra, R. 1999, AJ, 117, 3041
Hainaut, O. R., & Delsanti, A. C. 2002, A&A, 389, 641
Hall, S. M. 1997, MNRAS, 287, 148
Hendler, N., Pascucci, I., Pinilla, P., et al. 2020, ApJ, 895, 126
Jewitt, D. 2018, AJ, 155, 56
Jewitt, D., & Haghighipour, N. 2007, ARA&A, 45, 261
Jewitt, D. C., & Luu, J. X. 2001, AJ, 122, 2099
Jílková, L., Portegies Zwart, S., Pijloo, T., & Hammer, M. 2015, MNRAS,
Kobayashi, H., & Ida, S. 2001, Icar, 153, 416
Levison, H. F., Morbidelli, A., Van Laerhoven, C., Gomes, R., & Tsiganis, K.
  2008, Icar, 196, 258
Marsset, M., Fraser, W. C., Pike, R. E., et al. 2019, AJ, 157, 94
Marsset, M., Fraser, W. C., Schwamb, M. E., et al. 2023, PSJ, 4, 160
Morbidelli, A., Brown, M. E., & Levison, H. F. 2003, EM&P, 92, 1
Musielak, Z. E., & Quarles, B. 2014, RPPh, 77, 065901
Nesvorný, D., Vokrouhlický, D., Alexandersen, M., et al. 2020, AJ, 160, 46
Nesvorný, D., Vokrouhlický, D., & Deienno, R. 2014, ApJ, 784, 22
Öberg, K. I., Facchini, S., & Anderson, D. E. 2023, ARA&A, 61, 287
Olczak, C., Pfalzner, S., & Eckart, A. 2010, A&A, 509, A63
Parker, A. H., & Kavelaars, J. J. 2010, ApJL, 722, L204
Peixinho, N., Lacerda, P., & Jewitt, D. 2008, AJ, 136, 1837
Perotti, G., Christiaens, V., Henning, T., et al. 2023, Natur, 620, 516
Petit, J. M., Kavelaars, J. J., Gladman, B. J., et al. 2011, AJ, 142, 131
Petit, J. M., Kavelaars, J. J., Gladman, B. J., et al. 2017, AJ, 153, 236
Pfalzner, S. 2003, ApJ, 592, 986
Pfalzner, S., Bhandare, A., Vincke, K., & Lacerda, P. 2018, ApJ, 863, 45
Pfalzner, S., Govind, A., & Portegies Zwart, S. 2024a, NatAs, 8, 1380
Pfalzner, S., Govind, A., & Wagner, F. W. 2024b, ApJL, 972, L21
Pinilla-Alonso, N., Brunetto, R., De Prá, M. N., et al. 2025, NatAs, 9, 230
Pinilla-Alonso, N., Stansberry, J. A., & Holler, B. J. 2020, in The Trans-
  Neptunian Solar System, ed. D. Prialnik, M. A. Barucci, & L. Young
  (Amsterdam: Elsevier), 395
Raymond, S. N., Izidoro, A., Morbidelli, A., et al. 2020, Planetary
   Astrobiology (Tucson, AZ: Univ. Arizona Press)
Rein, H., & Spiegel, D. S. 2014, MNRAS, 446, 1424
Schwamb, M. E., Fraser, W. C., Bannister, M. T., et al. 2019, ApJS, 243, 12
Steinhausen, M., Olczak, C., & Pfalzner, S. 2012, A&A, 538, A10
Tegler, S. C., & Romanishin, W. 1998, Natur, 392, 49
Tegler, S. C., & Romanishin, W. 2000, Natur, 407, 979
Thirouin, A., & Sheppard, S. S. 2019, AJ, 158, 53
```

Vokrouhlický, D., Nesvorný, D., & Tremaine, S. 2024, ApJ, 968, 47